

160. Metal Complexes with Macrocyclic Ligands

Part XLVI¹⁾

Synthesis and Structures of Dinuclear Metal Complexes of Bis-macrocycles Having a Pyrazole Bridging Unit

by Harald Weller, Liselotte Siegfried, Markus Neuburger, Margareta Zehnder, and Thomas A. Kaden*

Institute of Inorganic Chemistry, Spitalstrasse 51, CH-4056 Basel

(31. VII. 97)

Three bis-macrocyclic ligands consisting of two N₃-, N₂S-, or NS₂-cyclononane rings, *i.e.*, of two octahydro-1*H*-1,4,7-triazonine, octahydro-1,4,7-thiadiazonine, or hexahydro-5*H*-1,4,7-dithiazonine rings, connected by a 1*H*-pyrazolediyl unit were prepared. They form dinuclear Cu^{II} and Ni^{II} complexes which are able to bind one additional exogenous bridging molecule such as Cl⁻, Br⁻, N₃⁻, SO₄²⁻, and 1*H*-pyrazol-1-ide. The structures determined by X-ray diffraction show that each Cu²⁺ is coordinated by the three donor atoms of the macrocyclic ring, by a pyrazolidodiyl N-atom, by an atom of the exogenous bridging ligand, and sometimes by a solvent molecule. In the majority of the Cu²⁺ cases, the metal ion exhibits square-pyramidal or trigonal-bipyramidal coordination geometry, except in the sulfato-bridged complex, in which one Cu²⁺ is hexacoordinated with the participation of a water molecule. The X-ray structure of the azide-bridged dinuclear Ni²⁺ complex was also solved and shows that both Ni²⁺ centres have octahedral coordination geometries. In all complexes, the 1*H*-pyrazolediyl group connecting the macrocycles is deprotonated and bridges the two metal centres, which, depending on the exogenous ligand, have distances between 3.6 and 4.5 Å. In the dinuclear Cu²⁺ complexes, antiferromagnetic coupling is present. The azido-bridged complex shows a very strong interaction with $-2J \geq 1040 \text{ cm}^{-1}$; in contrast, the 1*H*-pyrazol-1-ide and chloride bridged species have $-2J$ values of 300 and 272 cm⁻¹, respectively. Cyclic voltammetry of the Cu²⁺ complexes in MeCN reveals a strong dependence of the potentials Cu^{II}/Cu^I → Cu^{II}/Cu^I on the nature of the donor atoms of the macrocycle as well as on the type of bridging molecule. The more S-donors are present in the macrocycle, the higher is the potential, indicating a stabilization of the Cu^I oxidation state.

Introduction. – Over the past two decades, the bioinorganic chemistry of copper has been intensively studied on natural systems as well as using model compounds [2]. Especially interesting are di- and polynuclear proteins, such as haemocyanin (2 Cu²⁺) [3], laccase (4 Cu²⁺) [4], ascorbate oxidase (4 Cu²⁺) [5], or superoxide dismutase (Cu²⁺/Zn²⁺) [6] with regard to their structure and reactivity. In many of these systems, the metal centres are in close proximity to each other and are bridged by ligands.

Several dinuclear model complexes have been synthesized with the aim of mimicking this situation [7]. Often the metal centres are bridged either by endogenous (internal) or exogenous (external) ligands, which fix the complex in a predetermined geometry with a well-defined metal-metal distance. In these systems, therefore, the relationship between structural features and magnetic or electronic interactions can easily be studied and used to understand the often more complex biological systems.

¹⁾ Part XLV: [1].

In macrocyclic chemistry, different approaches for the formation of dinuclear complexes have been proposed. For example, mono- and bicyclic ligands with a large cavity can accommodate two metal ions [8]. Bis-macrocycles are another type of ligands which can form dinuclear metal complexes, in which the distance between the metal centres can be modulated through the length of the C-chain linking the two macrocycles [9]. The crystal structures of such complexes show that both the 'anti'- and the 'syn'(ear-muff)-configuration can be achieved, the latter, however, only when an exogenous bridging ligand is present to force the metal ions to adopt this configuration. The other possibility of obtaining the 'syn'-arrangement is to incorporate a bridging group into the linking chain. Endogenous bridging units such as alcoholate [10] or pyrazolide [11] have been used to force the complex into a preorganized structure. In addition to the endogenous bridging group, some of these complexes are able, additionally, to bind exogenous ligands. This makes them especially interesting as potential models for substrate recognition or as potential catalysts.

In continuation of such studies, we have improved the synthesis of **7** to an overall yield of 84%, using *N,N*-dimethylformamide dimethyl acetal to introduce a protecting group, have synthesized the two new bis-azathia-macrocycles **10** and **11**, and studied their dinuclear Cu^{2+} and Ni^{2+} complexes.

Experimental²⁾. – Compounds 1,4,7-triazatricyclo[5.2.1.0^{4,10}]decane (**1**) [12], octahydro-1,4,7-thiadiazonine (**2**) [13], hexahydro-5*H*-1,4,7-dithiazonine (**3**) [14], and 3,5-bis(chloromethyl)-1*H*-pyrazole hydrochloride (**4**) [15] were prepared according to the literature. UV/VIS: *Perkin-Elmer-Lambda-9* spectrophotometer; 0.9 mm solns. of the complex in H_2O . IR Spectra: *Perkin-Elmer-1600* spectrophotometer; KBr pellets. ¹H- and ¹³C-NMR Spectra: *Varian-Gemini-300* instrument; δ rel. to SiMe_4 as internal standard (= 0 ppm), *J* in Hz. Mass spectra: *Finnigan MAT 312*, FAB and EI; NBA = 3-nitrobenzyl alcohol. Elemental analyses were performed by the analytical laboratory of *Novartis* Basel.

1,1'-[(1*H*-Pyrazole-3,5-diyl)bis(methylene)]bis(1-azonia-4,7-diazatricyclo[5.2.1^{4,10}]decane) Dichloride (**5**). A suspension of **4** (1.48 g, 7.33 mmol) in MeCN was heated with Et_3N (7.4 ml, 1*M*) in MeCN and then filtered. This mixture was added over 15 min under N_2 at r.t. to **1** (2.04 g, 14.67 mmol), dissolved in abs. MeCN (30 ml), and heated to reflux for 2 h. After stirring overnight under N_2 at r.t., the soln. was filtered, the precipitate washed with Et_2O (3 \times), and dried at r.t. under h.v.: 2.66 g (84%). ¹H-NMR (CD_3OD): 3.18–3.75 (*m*, 12 CH_2N (macrocycle)); 3.8–3.9 (2*t*, 2 $\text{NCH}_2\text{-pyr}$); 5.98 (*s*, CH); 7.12 (*s*, CH (pyr)). ¹³C-NMR (CD_3OD): 49.7, 53.5, 58.20 (CH_2N); 58.8 ($\text{NCH}_2\text{-pyr}$); 113.0 (CH); 127.6 (pyr).

4,4'[(1*H*-Pyrazole-3,5-diyl)bis(methylene)]bis[octahydro-1*H*-1,4,7-triazonine-1-carbaldehyde] (**6**). A soln. of **5** (2.6 g, 6.02 mmol) in H_2O (40 ml) was refluxed for 20 h and then evaporated: 2.9 g (100%). ¹H-NMR (D_2O): 2.44–4.06 (*m*, 12 CH_2N (macrocycle)); 6.0–6.3 (*m*, pyr, 2 $\text{NCH}_2\text{-pyr}$); 7.81, 8.01 (2 *s*, 2 CHO). ¹³C-NMR (D_2O): 41.0, 43.6, 43.7, 43.8, 44.0, 44.4, 44.6, 46.5, 47.4, 48.5, 49.8, 49.9 (CH_2N); 50.6, 50.8 ($\text{NCH}_2\text{-pyr}$); 106.1, 143.0 (pyr); 166.9, 167.5 (CHO).

1,1'-[(1*H*-Pyrazole-3,5-diyl)bis(methylene)]bis[octahydro-1*H*-1,4,7-triazonine] Heptahydrochloride (**7** · 7 HCl). A soln. of **6** (2.9 g, 6.02 mmol) in H_2O (24 ml) and 36% HCl soln. (8 ml) was stirred for 2 h at 70–75° and 19 h at r.t. and then evaporated: 3.7 g (100%). ¹H-NMR (D_2O): 2.79 (*t*, 4 $\text{CH}_2\text{CH}_2\text{NCH}_2\text{-pyr}$); 3.13 (*t*, 4 $\text{CH}_2\text{CH}_2\text{NCH}_2\text{-pyr}$); 3.43 (*s*, 2 $\text{NCH}_2\text{CH}_2\text{N}$); 3.86 (*s*, 2 $\text{NCH}_2\text{-pyr}$); 6.63 (*s*, pyr). ¹³C-NMR (D_2O): 42.2, 43.6, 47.3 (CH_2N); 48.1 ($\text{NCH}_2\text{-pyr}$); 108.7, 143.7 (pyr).

Octahydro-1,4,7-thiadiazonine-4-carbaldehyde (**8**). *N,N*-Dimethylformamide dimethyl acetal (3.75 ml, 28.1 mmol) was added under N_2 to a soln. of **2** (3.79 g, 25.9 mmol) in abs. benzene (40 ml). The soln. was stirred for 15 min at r.t. and then heated within 30 min to 80°. The solvent was distilled off, and the residue hydrolyzed with $\text{EtOH}/\text{H}_2\text{O}$ 1:1 (160 ml) for 18 h at r.t. The solvent was evaporated, the remaining solid extracted with toluene (130 ml), the org. phase dried (Na_2SO_4) and evaporated, and the residue dried under h.v.: **8** (73%) as mixture of two isomers. IR: 3353*m* (NH), 2915*s* (CH_2), 1666*vs* (C=O), 1441 (*s*, CH_2). ¹H-NMR (CDCl_3): 1.80 (*br. s*, NH);

²⁾ Octahydro-1*H*-1,4,7-triazonine = 1,4,7-triazacyclononane, octahydro-1,4,7-thiadiazonine = 1,4-diaza-7-thiacyclononane, and hexahydro-5*H*-1,4,7-dithiazonine = 1-aza-4,7-dithiacyclononane.

2.43–3.85 (*m*, CH₂); 8.12, 8.20 (2 *s*, CHO). ¹³C-NMR (CDCl₃): 30.6, 31.2, 32.1, 36.3 (CH₂S); 45.3, 48.6, 48.7, 49.5, 49.9, 51.9, 53.1, 53.5 (CH₂N); 163.9, 164.2 (NCHO). EI-MS: 174 (*M*⁺).

General Alkylation Procedure: 9 and 11. To a mixture of **4** (8.88 mmol) and Na₂CO₃ (70 mmol); finely pulverized and dried for 1 h at 100°) in abs. MeCN (380 ml), **3** or **8** (18.70 mmol) in abs. MeCN (20 ml) was added under N₂. The mixture was stirred for 1 h at r.t. and then heated to reflux for 28 h. After removing the inorg. salts by filtration, the soln. was evaporated and the resulting oil dissolved in MeOH (10 ml). The soln. was filtered over a sintered-glass funnel G3 filled with silica gel (6 cm), and eluted with MeOH (150 ml). The org. phase was dried (Na₂SO₄), evaporated, and dried under h.v.

7,7'-[(1*H*-Pyrazole-3,5-diyl)bis(methylene)]bis[octahydro-1,4,7-thiadiazonine-4-carbaldehyde] (9): Yield 71%. IR: 3238*m* (br., NH), 3122*w* (=CH), 2918*s* (CH₂), 1666*vs* (C=O), 1572*w* (arom. C=C), 1442*s* (CH₂). ¹H-NMR (CDCl₃): 2.41–3.86 (*m*, CH₂N, CH₂S); 3.73 (*s*, CH₂-pyr); 6.08 (*s*, pyr); 8.05, 8.19 (2*s*, CHO). ¹³C-NMR (CDCl₃): 30.5, 31.3, 32.7, 35.9 (CH₂S); 48.1, 49.5, 49.7, 51.3, 52.8, 53.0, 55.2, 55.6, 59.1 (CH₂N); 104.3, 104.7 (pyr); 164.0 (CHO). CI-MS (NH₃): 441 (*[M + 1]*⁺).

7,7'-[(1*H*-Pyrazole-3,5-diyl)bis(methylene)]bis[hexahydro-5*H*-1,4,7-dithiazonine] (11): Yield 73%. IR: 3440*m* (NH), 2905*m* (CH₂), 1636*w* (arom. C=C), 1457*m* (CH₂). ¹H-NMR ((D₆)DMSO): 2.67 (*t*, ³J(H,H) = 4.7, SCH₂CH₂N); 2.87 (*t*, ³J(H,H) = 4.7, CH₂N); 3.10 (*s*, SCH₂CH₂S); 3.64 (*s*, CH₂-pyr); 6.11 (*s*, pyr). ¹³C-NMR ((D₆)DMSO): 32.1, 34.3 (CH₂S); 57.5 (CH₂N); 104.8 (pyr). CI-MS (NH₃): 419 (*[M + 1]*⁺). Anal. calc. for C₁₇H₃₀N₄S₄ · 1.97 HBr · 2.71 H₂O (626.96): C 32.57, H 6.01, Br 25.11, N 8.90, S 20.46, H₂O 7.79; found: C 32.87, H 5.92, Br 24.92, N 8.94, S 20.16, H₂O 7.51.

4,4'-[(1*H*-Pyrazole-3,5-diyl)bis(methylene)]bis[octahydro-1,4,7-thiadiazonine] (10). A mixture of **9** (2.50 g, 5.67 mmol) and 10% NaOH soln. (70 ml) was heated to reflux for 5 h under N₂ and filtered while hot. After cooling to 4° **10** precipitated. For further purification, the crude product was recrystallized from hot H₂O. 1.10 g (46%). IR: 3416*m* (NH), 3120*m* (=CH), 2917*m* (CH₂), 1637 and 1542*w* (arom. C=C), 1474*m* (CH₂). ¹H-NMR (CDCl₃): 2.50–3.08 (*m*, CH₂N, CH₂S); 3.80 (*s*, CH₂-pyr); 6.11 (*s*, pyr). ¹³C-NMR (CDCl₃): 32.4 (CH₂S); 46.3, 48.4, 52.6, 53.1, 53.5 (CH₂N); 102.6 (pyr). FAB-MS (NBA matrix): 385 (*[M + 1]*⁺). Anal. calc. for C₁₇H₃₂N₆S₂ · 3.86 H₂O (454.15): C 44.96, H 8.82, N 18.50, S 14.12, H₂O 15.31; found: C 44.97, H 8.89, N 18.55, S 14.02, H₂O 15.31.

μ-Azido{μ-{1,1'-[(1*H*-pyrazol-1-ido-3,5-diyl)bis(methylene)]bis[octahydro-1*H*-1,4,7-triazonine]}}dicopper (II) Bis(hexafluorophosphate) (12). See [11].

General Complexation Procedure: Dinuclear Copper (II) Complexes. To a soln. of the ligand **10** (0.2 mmol) in ROH/H₂O 1:1 (4 ml) or ligand **11** (0.2 mmol) in MeOH/CH₂Cl₂/H₂O 10:3:2 (15 ml), Cu(ClO₄)₂ · 5 H₂O (0.4 mmol) or CuCl₂/NH₄PF₆ (0.4 mmol) and the bridging ligand (0.2 mmol) were added. The soln. was heated for 10 min at 50°. After cooling, the complex was collected by filtration, washed with a small amount of H₂O, and finally dried in the desiccator.

μ-Azido{μ-{4,4'-[(1*H*-pyrazol-1-ido-3,5-diyl)bis(methylene)]bis[octahydro-1,4,7-thiadiazonine]}}dicopper (II) Bis(hexafluorophosphate) (13a): Yield 40%. IR: 3424*m* (NH), 2929*w* (CH₂), 2049*s* (N₃), 1636*w* (arom. C=C), 838*s* (PF₆⁻). Anal. calc. for C₁₇H₃₁Cu₂F₁₂N₆P₂S₂ · 0.15 CH₃OH (847.44): C 24.31, H 3.76, Cu 15.0, F 26.90, N 14.88, S 7.57; found: C 24.62, H 3.60, Cu 15.0, F 27.21, N 14.90, S 7.40.

μ-(1*H*-Pyrazol-1-ido){μ-{4,4'-[(1*H*-pyrazol-1-ido-3,5-diyl)bis(methylene)]bis[octahydro-1,4,7-thiadiazonine]}}dicopper (II) Diperchlorate (13b): Yield 60%. IR: 3445*m* (NH), 2927*w* (CH₂), 1624*w* (arom. C=C), 1080*vs* (ClO₄⁻). FAB-MS (NBA matrix): 677 ([M₂LZ – ClO₄⁻]⁺), 609 ([M₂LZ – pyr – ClO₄⁻]⁺), 576 ([M₂LZ – 2 ClO₄⁻]⁺), 509 ([M₂LZ – pyr – 2 ClO₄⁻]⁺). Anal. calc. for C₂₀H₃₄Cl₂Cu₂N₆O₈S₂ · 0.62 H₂O (787.84): C 30.49, H 4.51, Cl 9.00, Cu 16.1, N 14.22, S 8.14, H₂O 1.42; found: C 30.67, H 4.51, Cl 8.97, Cu 15.7, N 14.33, S 8.00, H₂O 1.42.

μ-Sulfato{μ-{4,4'-[(1*H*-pyrazol-1-ido-3,5-diyl)bis(methylene)]bis[octahydro-1,4,7-thiadiazonine]}}dicopper (II) Hexafluorophosphate (13c): Yield 40%. IR: 3431*m* (NH), 2931*w* (CH₂), 1636*w* (arom. C=C), 1182, 1118, 1041*m* (SO₄²⁻ bridge), 988*w* (SO₄²⁻), 842*s* (PF₆⁻). FAB-MS (NBA matrix): 607 ([M₂LZ – PF₆⁻]⁺), 509 ([M₂LZ – SO₄²⁻ – PF₆⁻]⁺). Anal. calc. for C₁₇H₃₁Cu₂F₆N₆O₄PS₃ · 3 H₂O (805.76): C 25.34, H 4.62, N 10.43, S 11.94; found: C 25.35, H 4.47, N 10.73, S 11.52.

μ-Chloro{μ-{4,4'-[(1*H*-pyrazol-1-ido-3,5-diyl)bis(methylene)]bis[hexahydro-5*H*-1,4,7-dithiazonine]}}dicopper (II) Diperchlorate (14a): Yield 30%. IR: 3424*m* (NH), 2923*m* (CH₂), 1636*w* (arom. C=C), 1457*w* (CH₂), 1121*vs* (ClO₄⁻). FAB-MS (NBA matrix): 679 ([M₂LZ – ClO₄⁻]⁺), 644 ([M₂LZ – Cl⁻ – ClO₄⁻]⁺), 580 ([M₂LZ – 2 ClO₄⁻]⁺), 543 ([M₂LZ – Cl⁻ – 2 ClO₄⁻]⁺). Anal. calc. for C₁₇H₂₉Cl₃Cu₂N₄O₈S₄ · 0.5 CH₃OH · 0.83 H₂O (810.11): C 25.95, H 4.06, Cl 13.13, Cu 15.7, N 6.92, S 15.83, H₂O 1.85; found: C 25.70, H 3.99, Cl 13.16, Cu 15.5, N 7.06, S 15.75, H₂O 1.89.

μ-Bromo{μ-{4,4'-[(1*H*-pyrazol-1-ido-3,5-diyl)bis(methylene)]bis[hexahydro-5*H*-1,4,7-dithiazonine]}}dicopper (II) Diperchlorate (14b): Yield 30%. IR: 3420*m* (NH), 2922*w* (CH₂), 1636*w* (arom. C=C), 1471*w* (CH₂),

1120vs (ClO_4^-). Anal. calc. for $\text{C}_{17}\text{H}_{29}\text{BrCl}_2\text{Cu}_2\text{N}_4\text{O}_8\text{S}_4 \cdot \text{H}_2\text{O}$ (841.66): C 24.26, H 3.71, Cl 8.42, N 6.66, S 15.24, H_2O 2.1; found: C 24.49, H 3.65, Cl 8.83, N 6.79, S 14.89, H_2O 2.1.

μ -Azido{ μ -{1,1'-[[1H-pyrazol-1-ido-3,5-diyl]bis(methylene)]bis[octahydro-1H-1,4,7-triazonine]}}dinickel (II) Diperchlorate (15). To a suspension of **7** (379.4 mg, 1.08 mmol) in MeOH (20 ml) at 60°, a soln. of $\text{Ni}(\text{ClO}_4)_2 \cdot 6 \text{H}_2\text{O}$ (790 mg, 2.16 mmol) in MeOH (20 ml) was added over 15 min. Then H_2O was added until a clear soln. was obtained. After addition of MeONa (5 ml, 0.2N), the soln. was stirred for 10 min, filtered, and evaporated. The product was purified over a *Sephadex G10* (10 g, column *Pharmacia*) by elution with H_2O . The 3rd fraction gave 300 mg (38%) of violet crystals. UV/VIS: 900 (sh), 550 (27). IR: 2921 (CH_2), 1638 (arom. C=C), 1080 (ClO_4^-). FAB-MS (NBA matrix): 665 ($[\text{M}_2\text{LZ} - 2 \text{ClO}_4^-]^+$), 463 ($[\text{M}_2\text{LZ} - 3 \text{ClO}_4^-]^+$).

To the so obtained complex (0.13 mmol), dissolved in EtOH (3 ml) and H_2O (0.5 ml), NaN_3 (0.13 mmol) was added and the mixture heated to 60° for 5 min. Diffusion of Et_2O into the EtOH/ H_2O soln. yielded 60 mg (62%) of dark blue crystals. UV/VIS: 933 (68), 559 (33), 325 (299). IR: 2926w (CH_2), 2052s (N_3^-), 1633w (arom. C=C), 1074 (ClO_4^-). FAB-MS (NBA matrix): 665 ($[\text{M}_2\text{LZ} - \text{N}_3^-]^+$), 608 ($[\text{M}_2\text{LZ} - \text{ClO}_4^-]^+$), 565 ($[\text{M}_2\text{LZ} - \text{ClO}_4^- - \text{N}_3^-]^+$), 507 ($[\text{M}_2\text{LZ} - 2 \text{ClO}_4^-]^+$), 463 ($[\text{M}_2\text{LZ} - 2 \text{ClO}_4^- - \text{N}_3^-]^+$).

μ -Azido{ μ -{1,1'-[[1H-pyrazol-1-ido-3,5-diyl]bis(methylene)]bis[octahydro-1,4,7-thiadiazonine]}}dinickel (II) Diperchlorate (16). To a soln. of **10** (37.5 mg, $8.5 \cdot 10^{-5}$ mol) in EtOH/ H_2O 1:1 (4 ml), $\text{Ni}(\text{ClO}_4)_2 \cdot 6 \text{H}_2\text{O}$ (77.0 mg, $2.1 \cdot 10^{-4}$ mol) and NaOH ($1.0 \cdot 10^{-4}$ mol) were added. The blue soln. of the complex was treated with NaN_3 ($8.5 \cdot 10^{-5}$ mol) in H_2O (1 ml), then heated to 60° for 50 min, filtered, and evaporated. The residue was dissolved in EtOH/ H_2O 1:1 (2 ml) and filtered. Standing on air yielded violet crystals. Yield 30%. IR: 2926w (CH_2), 2055s (N_3^-), 1636w (arom. C=C), 1116 (ClO_4^-). FAB-MS (NBA matrix): 699 ($[\text{M}_2\text{LZ} - \text{N}_3^-]^+$), 642 ($[\text{M}_2\text{LZ} - \text{ClO}_4^-]^+$), 599 ($[\text{M}_2\text{LZ} - \text{ClO}_4^- - \text{N}_3^-]^+$), 540 ($[\text{M}_2\text{LZ} - 2 \text{ClO}_4^-]^+$), 497 ($[\text{M}_2\text{LZ} - 2 \text{ClO}_4^- - \text{N}_3^-]^+$).

X-Ray Diffraction Measurements. The crystal data and parameters of the data collection for the Cu^{2+} complexes **13c**, **14a**, and **14b**, as well as for the Ni^{2+} complex **15** are given in *Table 1*. Complex **13c** was measured in the presence of the mother liquor MeOH/ H_2O because of a decreasing quality of the crystals on standing in the air. Unit-cell parameters were determined by accurate centering of 25 independent strong reflections by the least-squares method. Three standard reflections monitored every 2 h during data collection showed no significant variation of the intensity. The raw data set was corrected for polarization effects and X-ray diffraction absorption. The structure was solved by direct methods [16]. Anisotropic least-squares refinements were carried out on all non-H-atoms, using the program CRYSTALS [17]. In **13c**, the PF_6^- ion, and in **15**, the ClO_4^- ion is disordered. They were refined using two split positions per atom keeping the sum of their occupancy equal to 1. H-Atoms are in calculated positions with C–H distances of 0.96 Å and fixed isotropic thermal parameters. Scattering factors are taken from [18].

Magnetic Measurements. The temperature dependence of the molar magnetic susceptibility of compounds **13a**, **13b**, and **14a** was measured between 1.7 and 400 K at 5000 G in a *Suprasil* quartz tube with a *SQUID* magnetometer *MPMS 5S* (*Quantum Design*, San Diego). Diamagnetic corrections were done using the values tabulated in [19].

Cyclic Voltammetry. Voltammetric experiments were performed with a three-electrode cell composed of 'glassy carbon' working and auxiliary electrodes and a Ag/AgCl reference electrode. Voltammograms were recorded with an *Eco Chemie Autolab PGSTAT 20* potentiostat controlled via *GPES 3.2* software on a PC 386 computer. Potentials were corrected against an internal ferrocene standard (E_0 400 mV vs. NHE) added at the end of each experiment. MeCN, freshly distilled over P_4O_{10} , was used as solvent and $(\text{Bu}_4\text{N})\text{BF}_4$ (0.1M), recrystallized twice from EtOH/ H_2O and dried *in vacuo* over P_4O_{10} as supporting electrolyte. All electrochemical experiments were done at 25° in solns. deaerated by bubbling N_2 through them.

Results and Discussion. – *Synthesis.* The syntheses of the three bis-macrocylic ligands **7**, **10**, and **11** were carried out by *N*-alkylations of the corresponding macrocycles **1**, **3**, and **8** with 3,5-bis(chloromethyl)-1H-pyrazole hydrochloride (**4**) as bifunctional alkylating agent (see *Scheme*).

For the preparation of **7** and **10**, the selective protection of two or one N-atom of the macrocycle was required. Both were achieved using *N,N*-dimethylformamide dimethyl acetal as protecting agent [12] [20]. In the case of **7**, **4** was reacted directly with the tricyclic orthoamide **1** to give the salt **5**, followed by hydrolysis first to **6** and then to **7**. This new synthesis is easier and gives better yields than the one previously described [11]. Compound **10** was synthesized by reacting the corresponding mono-

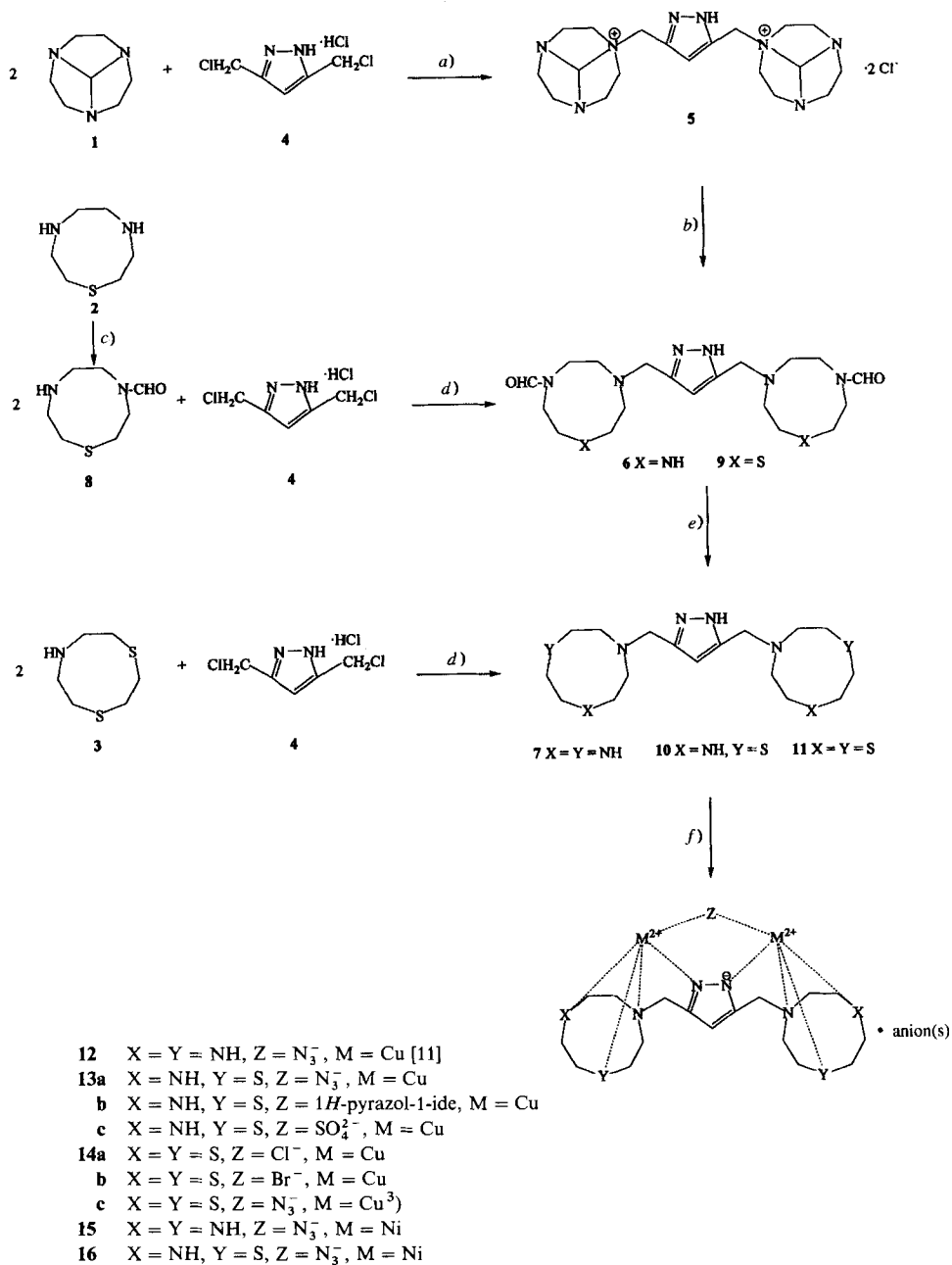
Table 1. Crystal Data and Parameter of Data Collection for the Cu^{2+} Complexes **13c**, **14a**, and **14b** and the Ni^{2+} Complex **15**

	13c	14a	14b	15
Formula	$\text{C}_{17}\text{H}_{29}\text{Cu}_2\text{N}_6\text{O}_4\text{S}_3 \cdot \text{PF}_6 \cdot \text{CH}_3\text{OH} \cdot 3 \text{H}_2\text{O}$	$\text{C}_{17}\text{H}_{29}\text{ClCu}_2\text{N}_4\text{S}_4 \cdot 2 \text{ClO}_4 \cdot \text{CH}_3\text{CN}$	$\text{C}_{17}\text{H}_{29}\text{BrCu}_2\text{N}_4\text{S}_4 \cdot 2 \text{ClO}_4 \cdot \text{H}_2\text{O}$	$\text{C}_{17}\text{H}_{29}\text{N}_{11}\text{Ni}_2 \cdot 3 \text{H}_2\text{O} \cdot 2 \text{ClO}_4$
Mol. wt.	835.79	820.17	841.60	757.859
Crystal system	triclinic	monoclinic	orthorhombic	monoclinic
Space group	$P\bar{1}$	$P2_1/n$	$Pbca$	$P2_1/c$
a [Å]	7.9681(8)	10.974(1)	13.129(4)	10.538(4)
b [Å]	13.2943(20)	10.750(1)	14.855(6)	15.396(10)
c [Å]	15.8592(27)	25.929(3)	29.155(6)	18.741(8)
α [deg]	93.7(7)	90	90	90.00
β [deg]	93.2(6)	95.820(9)	90	98.72(5)
γ [deg]	98.5(6)	90	90	90.00
Volume [Å ³]	1654.6(4)	3043.0(5)	5686(3)	3005(3)
Z	2	4	8	4
$F(000)$	856	1672	3392	1568
Density [gcm ⁻³]	1.68	1.79	1.96	1.675
μ [mm ⁻¹]	4.54	7.19	3.42	3.84
Crystal size [mm]	0.11 × 0.46 × 0.66	0.28 × 0.40 × 0.48	0.20 × 0.35 × 0.50	0.18 × 0.34 × 0.42
Temperature [K]	293	293	293	293
Radiation	CuK_α (λ 1.54178)	CuK_α (λ 1.54180)	MoK_α (λ 0.71069)	CuK_α (λ 1.54180)
Scan type	$\omega/2\theta$	$\omega/2\theta$	$\omega/2\theta$	$\omega/2\theta$
θ_{max} [°]	66.74	77.50	28.47	77.50
No. of measured refl.	6323	6554	7793	11359
No. of indep. refl.	5860	6048	7091	5876
No. of refl. in ref.	4633	5468	2758	4224
No. of variables	476	371	352	472
Final R value [%]	5.75	4.77	4.72	5.94
Final R_w value [%]	6.96	5.87	4.08	7.07
Weighting scheme	Chebychev [23]	Chebychev [23]	Chebychev [23]	Chebychev [23]

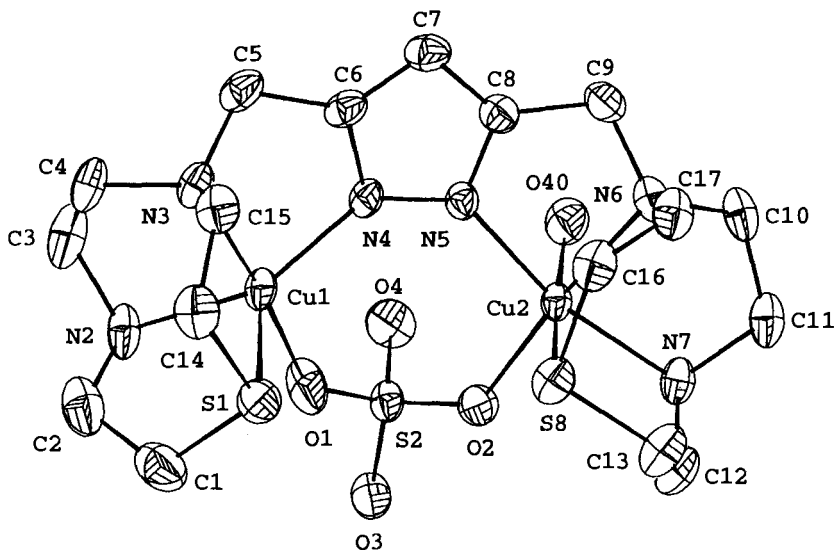
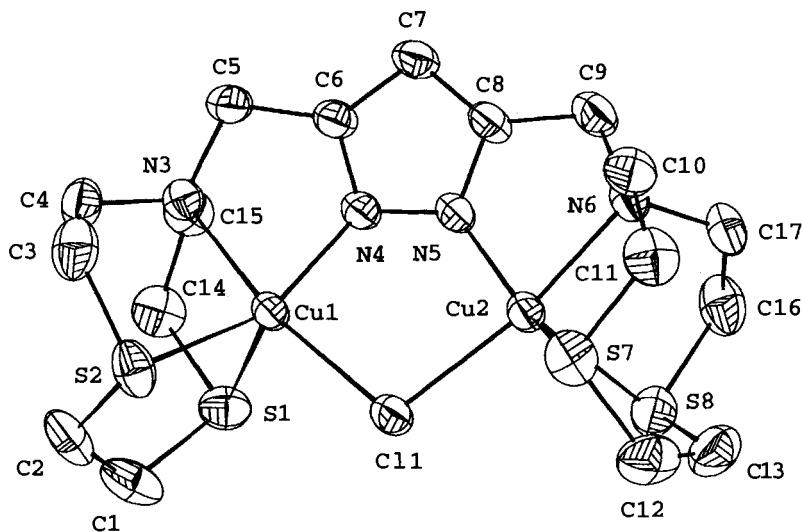
formyl-protected macrocycle **8**, which was obtained after hydrolysis of the intermediate cyclic aminal in 71% yield. For hexahydro-5*H*-1,4,7-dithiazonine (**3**) of course, no protection was needed. The removal of the CHO groups of **6** and **9** was carried out in the presence of acid or under basic conditions, respectively. All three ligands gave dinuclear Cu^{2+} and Ni^{2+} complexes, the properties of which were studied.

Structures. The X-ray structures of the dinuclear Cu^{2+} complexes **13c**, **14a**, and **14b** are shown in Figs. 1–3. In all these structures, each Cu^{2+} is coordinated by the three donor atoms of the macrocycle, one pyrazolidodiyl N-atom and one atom of the exogenous bridging ligand. Remarkably, the dinuclear Cu^{2+} complex **13c** has two different coordination geometries with different coordination numbers at each copper site. The coordination geometry of Cu(1) is distorted trigonal-bipyramidal with N(3) and O(1) of the sulfato-bridge in the axial positions. In contrast, Cu(2) exhibits a distorted octahedral coordination with an additional O-atom (O(40)) of a water molecule in the sixth position. The deviations from the best plane through N(5), N(6), N(7), and O(2) are ± 0.02 Å, the central ion being located 0.05 Å out of this plane. The bond lengths between the Cu^{2+} centres and the pyrazolidodiyl N-atoms are slightly shorter (*ca.* 0.1 Å) than normal Cu–N bond lengths, due to the influence of the negative charge on the pyrazole moiety. The Cu(1)–Cu(2) distance is 4.16 Å (Table 2).

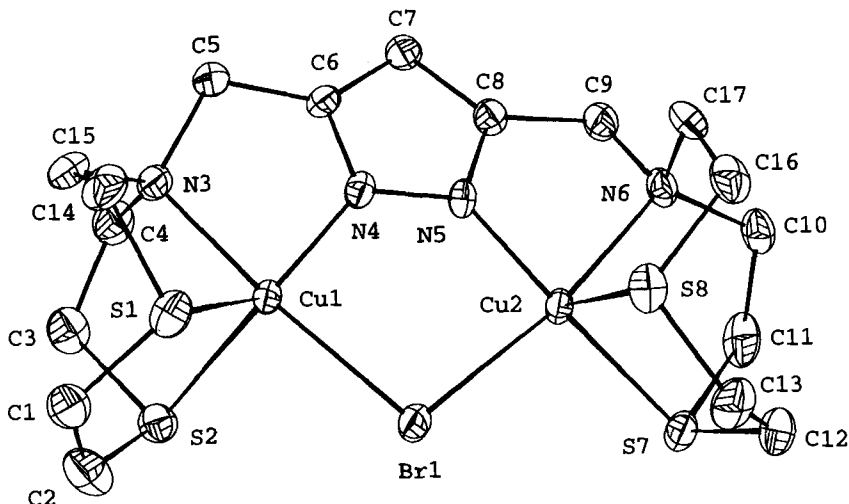
Scheme



a) 1 Equiv. Et₃N, MeCN, 80°, 2 h. *b*) H₂O, 100°, 24 h. *c*) 1) *N,N*-Dimethylformamide dimethyl acetal, benzene, 80°, 30 min; 2) EtOH/H₂O. *d*) Na₂CO₃, MeCN, 80°, 28 h. *e*) 10% NaOH, soln. 100°, 5 h (**10**); 3*N* HCl, 70%, 2 h (**7**). *f*) 2M^{II} (anion)₂, Z.

Fig. 1. ORTEP Plot of **13c**. Arbitrary numbering.Fig. 2. ORTEP Plot of **14a**. Arbitrary numbering.

The structures of **14a** and **14b** are very similar to each other. They show distorted trigonal-bipyramidal coordination geometries around each Cu^{2+} ion. One axial site of each bipyramid is occupied by the bridging halogenide, the other one by the atoms N(3) and N(6), respectively. In these complexes too, the negative charge of the pyrazolidodiyil N-atoms results in slightly shorter bonds to the corresponding Cu^{2+} centre (Tables 3 and 4). The Cu(1)–Cu(2) distances in the halogenide-bridged complexes are almost identical (3.70 Å for **14a** and 3.76 Å for **14b**).

Fig. 3. ORTEP Plot of **14b**. Arbitrary numbering.Table 2. Selected Bond Lengths [Å] and Angles [°] of **13c**. For numbering, see Fig. 1.

Cu(1)–Cu(2)	4.156(1)	Cu(2)–O(40)	2.600(4)
Cu(1)–O(1)	1.947(4)	Cu(2)–O(2)	1.987(3)
Cu(1)–S(1)	2.529(1)	Cu(2)–S(8)	2.596(1)
Cu(1)–N(2)	2.007(4)	Cu(2)–N(7)	2.019(4)
Cu(1)–N(3)	2.076(4)	Cu(2)–N(6)	2.071(4)
Cu(1)–N(4)	1.926(4)	Cu(2)–N(5)	1.951(3)
Cu(1)–O(1)–S(2)	139.6(3)	Cu(2)–O(2)–S(2)	132.1(2)
S(1)–Cu(1)–O(1)	96.2(2)	S(8)–Cu(2)–O(2)	95.2(1)
N(2)–Cu(1)–O(1)	89.6(2)	N(7)–Cu(2)–O(2)	90.5(2)
S(1)–Cu(1)–N(2)	87.9(2)	N(7)–Cu(2)–S(8)	85.7(1)
N(3)–Cu(1)–O(1)	172.8(2)	N(6)–Cu(2)–O(2)	173.3(2)
S(1)–Cu(1)–N(3)	87.1(1)	N(6)–Cu(2)–S(8)	88.2(1)
N(2)–Cu(1)–N(3)	84.1(2)	N(6)–Cu(2)–N(7)	83.9(2)
N(4)–Cu(1)–O(1)	102.5(1)	N(5)–Cu(2)–O(2)	103.1(1)
S(1)–Cu(1)–N(4)	111.8(1)	N(5)–Cu(2)–S(8)	95.6(1)
N(2)–Cu(1)–N(4)	155.2(2)	N(5)–Cu(2)–N(7)	166.1(2)
N(3)–Cu(1)–N(4)	82.1(2)	N(5)–Cu(2)–N(6)	82.3(2)
		S(8)–Cu(2)–O(40)	177.8(1)
		N(7)–Cu(2)–O(40)	92.8(1)
		N(6)–Cu(2)–O(40)	90.0(1)
		N(5)–Cu(2)–O(40)	85.4(1)
		O(2)–Cu(2)–O(40)	86.5(1)

The structure of the dinuclear Ni^{2+} complex **15** shows two hexacoordinate metal centres (Fig. 4). The three donors of the octahydro-1*H*-1,4,7-triazonine moiety, an N-atom from the pyrazolide, and one of the bridging azide, as well as a H_2O molecule coordinate each metal ion to give a distorted octahedral geometry. Interestingly, in contrast to the structures of the Cu^{2+} complexes discussed above, the arrangement of the

Table 3. Selected Bond Lengths [Å] and Angles [°] of **14a**. For numbering, see Fig. 2.

Cu(1)–Cu(2)	3.697(1)		
Cu(1)–Cl(1)	2.3731(8)	Cu(2)–Cl(1)	2.3589(7)
Cu(1)–S(1)	2.4650(8)	Cu(2)–S(8)	2.4384(8)
Cu(1)–S(2)	2.3336(8)	Cu(2)–S(7)	2.3511(8)
Cu(1)–N(3)	2.128(2)	Cu(2)–N(6)	2.135(2)
Cu(1)–N(4)	1.886(2)	Cu(2)–N(5)	1.877(2)
Cu(1)–Cl(1)–Cu(2)	102.76(3)		
Cl(1)–Cu(1)–S(1)	98.26(3)	Cl(1)–Cu(2)–S(8)	103.01(3)
Cl(1)–Cu(1)–S(2)	101.67(3)	Cl(1)–Cu(2)–S(7)	95.31(3)
S(1)–Cu(1)–S(2)	89.59(3)	S(7)–Cu(2)–S(8)	90.42(3)
Cl(1)–Cu(1)–N(3)	168.90(7)	Cl(1)–Cu(2)–N(6)	169.88(7)
S(1)–Cu(1)–N(3)	86.12(7)	N(6)–Cu(2)–S(8)	86.51(7)
S(2)–Cu(1)–N(3)	88.50(7)	N(6)–Cu(2)–S(7)	87.95(7)
Cl(1)–Cu(1)–N(4)	89.07(7)	Cl(1)–Cu(2)–N(5)	90.15(7)
S(1)–Cu(1)–N(4)	121.88(9)	N(5)–Cu(2)–S(8)	128.48(8)
S(2)–Cu(1)–N(4)	145.16(9)	N(5)–Cu(2)–S(7)	138.31(9)
N(3)–Cu(1)–N(4)	79.98(9)	N(5)–Cu(2)–N(6)	81.1(1)

Table 4. Selected Bond Lengths [Å] and Angles [°] of **14b**. For numbering, see Fig. 3.

Cu(1)–Cu(2)	3.760(1)		
Cu(1)–Br(1)	2.482(1)	Cu(2)–Br(1)	2.488(1)
Cu(1)–S(1)	2.429(2)	Cu(2)–S(8)	2.492(2)
Cu(1)–S(2)	2.350(2)	Cu(2)–S(7)	2.302(2)
Cu(1)–N(3)	2.120(6)	Cu(2)–N(6)	2.107(6)
Cu(1)–N(4)	1.875(6)	Cu(2)–N(5)	1.885(6)
Cu(1)–Br(1)–Cu(2)	98.33(4)		
Br(1)–Cu(1)–S(1)	101.59(6)	Br(1)–Cu(2)–S(8)	96.75(6)
Br(1)–Cu(1)–S(2)	94.75(6)	Br(1)–Cu(2)–S(7)	100.87(6)
S(1)–Cu(1)–S(2)	90.89(9)	S(7)–Cu(2)–S(8)	90.32(8)
Br(1)–Cu(1)–N(3)	170.8(2)	Br(1)–Cu(2)–N(6)	170.0(2)
S(1)–Cu(1)–N(3)	87.5(2)	N(6)–Cu(2)–S(8)	86.4(2)
S(2)–Cu(1)–N(3)	86.7(2)	N(6)–Cu(2)–S(7)	88.6(2)
Br(1)–Cu(1)–N(4)	91.4(2)	Br(1)–Cu(2)–N(5)	90.1(2)
S(1)–Cu(1)–N(4)	128.2(2)	N(5)–Cu(2)–S(8)	115.1(2)
S(2)–Cu(1)–N(4)	138.2(2)	N(5)–Cu(2)–S(7)	151.1(2)
N(3)–Cu(1)–N(4)	81.5(2)	N(5)–Cu(2)–N(6)	80.0(2)

two facially coordinated macrocycles, and, therefore, also of the two H₂O molecules, is 'transoid'. The Ni–N bonds are in their normal range, and the Ni(1)–Ni(2) distance is 4.45 Å (Table 5).

Magnetic Properties. The magnetic moments of the complexes **13a**, **13b**, and **14a** at room temperature are lower than expected for two independent paramagnetic Cu²⁺ ions, indicative of an antiferromagnetic coupling. The temperature dependence of the magnetic susceptibility χ_{mol} was measured and fitted to the *Bleaney-Bowers* expression (Eqn. 1) [21], using the

$$\chi_{\text{mol}} = \frac{N\beta^2 g^2}{3kT} \cdot \left(1 + \frac{1}{3} e^{-\frac{2J}{kT}}\right)^{-1} \cdot (1 - \rho) + \frac{N\beta^2 g^2}{4kT} \cdot \rho + N_A \quad (1)$$

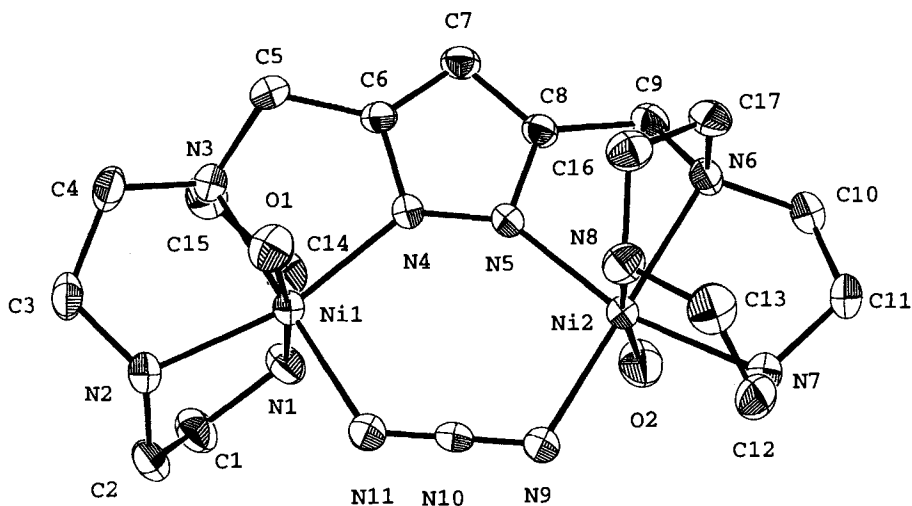


Fig. 4. ORTEP Plot of 15. Arbitrary numbering.

Table 5. Selected Bond Lengths [Å] and Angles [°] of 15. For numbering, see Fig. 4.

Ni(1)–Ni(2)	4.450(1)	Ni(2)–O(2)	2.167(3)
Ni(1)–O(1)	2.161(3)	Ni(2)–N(6)	2.121(3)
Ni(1)–N(1)	2.093(3)	Ni(2)–N(7)	2.086(4)
Ni(1)–N(2)	2.097(3)	Ni(2)–N(8)	2.074(4)
Ni(1)–N(3)	2.115(3)	Ni(2)–N(5)	2.041(3)
Ni(1)–N(4)	2.041(3)	Ni(2)–N(9)	2.106(4)
Ni(1)–N(11)	2.102(4)		
Ni(1)–N(11)–N(10)	119.7(3)	Ni(2)–N(9)–N(10)	117.5(3)
N(1)–Ni(1)–N(11)	94.3(2)	N(8)–Ni(2)–N(9)	93.3(3)
N(2)–Ni(1)–N(11)	96.3(1)	N(7)–Ni(2)–N(9)	95.6(1)
N(1)–Ni(1)–N(2)	83.5(1)	N(7)–Ni(2)–N(8)	83.7(2)
N(3)–Ni(1)–N(11)	177.9(1)	N(6)–Ni(2)–N(9)	176.7(2)
N(1)–Ni(1)–N(3)	83.6(1)	N(6)–Ni(2)–N(8)	83.4(1)
N(2)–Ni(1)–N(3)	83.8(1)	N(6)–Ni(2)–N(7)	83.4(1)
N(4)–Ni(1)–N(11)	98.5(1)	N(5)–Ni(2)–N(9)	99.5(1)
N(1)–Ni(1)–N(4)	96.3(1)	N(5)–Ni(2)–N(8)	95.9(1)
N(2)–Ni(1)–N(4)	165.2(1)	N(5)–Ni(2)–N(7)	164.9(1)
N(3)–Ni(1)–N(4)	81.5(1)	N(5)–Ni(2)–N(6)	81.6(1)
N(1)–Ni(1)–O(1)	172.6(1)	N(8)–Ni(2)–O(2)	173.5(1)
N(2)–Ni(1)–O(1)	89.9(1)	N(7)–Ni(2)–O(2)	90.3(1)
N(3)–Ni(1)–O(1)	92.4(1)	N(6)–Ni(2)–O(2)	93.3(1)
N(4)–Ni(1)–O(1)	89.2(1)	N(5)–Ni(2)–O(2)	89.2(1)
N(11)–Ni(1)–O(1)	89.7(2)	N(9)–Ni(2)–O(2)	89.9(2)

isotropic (Heisenberg) exchange Hamiltonian ($H = -2JS_1S_2$) for two interacting $S = 1/2$ centres. χ_{mol} is expressed per mol of Cu-atom, N_a is the temperature-independent paramagnetism, and ρ the fraction of paramagnetic impurity. The other symbols have their usual meaning.

The experimental data were least-squares fitted to the theoretical expression, keeping the value of g constant and all other parameters variable (Table 6). The spin exchange within the complex is highly dependent on the nature of the exogenous bridge. The azide-bridged complex **13a** exhibits a low magnetic susceptibility over a wide temperature range (Fig. 5). At very low temperatures, a small but significant amount of paramagnetic impurity is observed. Both the high $-2J$ value ($\geq 1038 \text{ cm}^{-1}$) and the low magnetic moment $\mu = 0.47 \text{ BM}$ at room temperature indicate a very strong antiferromagnetic coupling. The temperature dependence of χ_{mol} for **13b** and **14a** (Figs. 6 and 7) allows the determination of the values $-2J = 300 \text{ cm}^{-1}$ for **13b** and $2J = 272 \text{ cm}^{-1}$ for **14a**. The two complexes behave similarly and demonstrate antiferromagnetic coupling only at low temperature, whereas at 300 K the magnetic moments are 1.42 and 1.37 BM, respectively.

Table 6. Magnetic Parameters Obtained from the Temperature Dependence of χ_{mol} for Complexes **13a**, **13b**, and **14a**

	g	$-2J [\text{cm}^{-1}]$	$N_a [10^6 \text{ cm}^3 \text{ mol}^{-1}]$	ρ	$\mu_{\text{eff}} [\text{BM}]$ at 300 K
13a	2.1 ^{a)}	≥ 1038	51	$5.9 \cdot 10^{-3}$	0.47
13b	2.1 ^{a)}	300	37	–	1.42
14a	2.0 ^{a)}	272	52	$2.3 \cdot 10^{-2}$	1.37

^{a)} Kept constant during the fitting procedure.

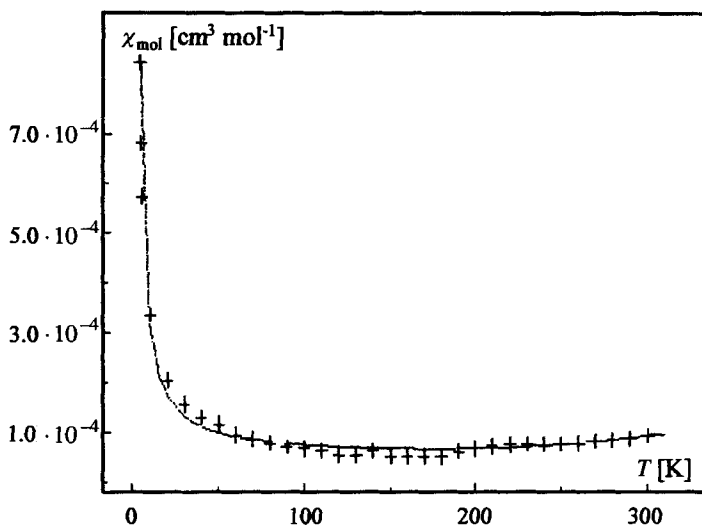


Fig. 5. Temperature dependence of the corrected molar magnetic susceptibility (χ_{mol}) of **13a** ($\sigma(Y) = 1.6 \cdot 10^{-5}$). Experimental points, +; calculated curve, —.

Electrochemistry. The cyclic voltammetry of the dinuclear Cu^{2+} complexes is characterized by two one-electron processes due to two reduction and two oxidation steps, respectively (Fig. 8). They describe the quasi-reversible redox transitions $\text{Cu}^{\text{II}}/\text{Cu}^{\text{I}} \rightarrow \text{Cu}^{\text{II}}/\text{Cu}^{\text{I}}$ (a) and $\text{Cu}^{\text{II}}/\text{Cu}^{\text{I}} \rightarrow \text{Cu}^{\text{I}}/\text{Cu}^{\text{I}}$ (b) in both directions. The differences be-

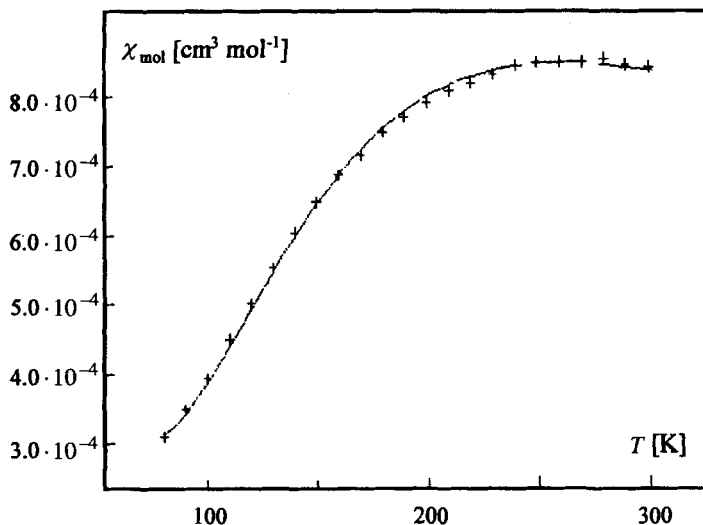


Fig. 6. Temperature dependence of the corrected molar magnetic susceptibility (χ_{mol}) of **13b** ($\sigma(Y) = 7.3 \cdot 10^{-6}$). Experimental points, +; calculated curve, -.

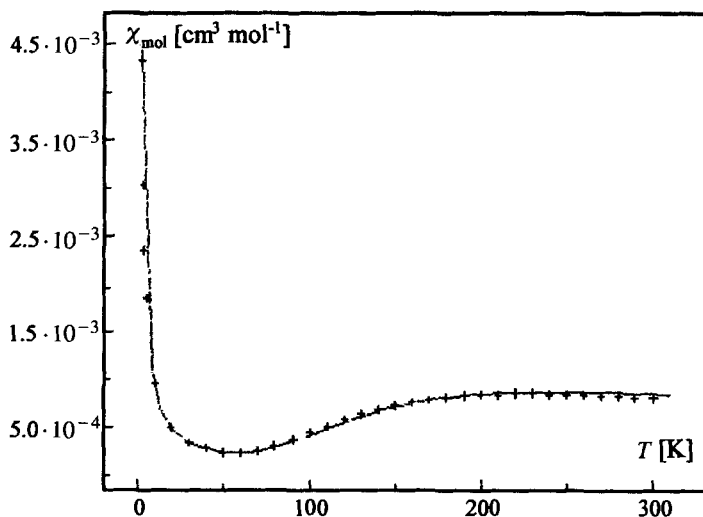


Fig. 7. Temperature dependence of the corrected molar magnetic susceptibility (χ_{mol}) of **14a** ($\sigma(Y) = 3.7 \cdot 10^{-5}$). Experimental points, +; calculated curve, -.

tween $E_{1/2}(\text{a})$ and $E_{1/2}(\text{b})$ are between 220 and 252 mV and are clearly larger than the statistical value of 35.6 mV expected for two independent Cu^{2+} centres [22]. Comparing the redox potentials of the different complexes, a strong dependence on the nature of the donor atoms of the bis-macrocycle as well as on the type of bridging ligand can be observed (Table 7).

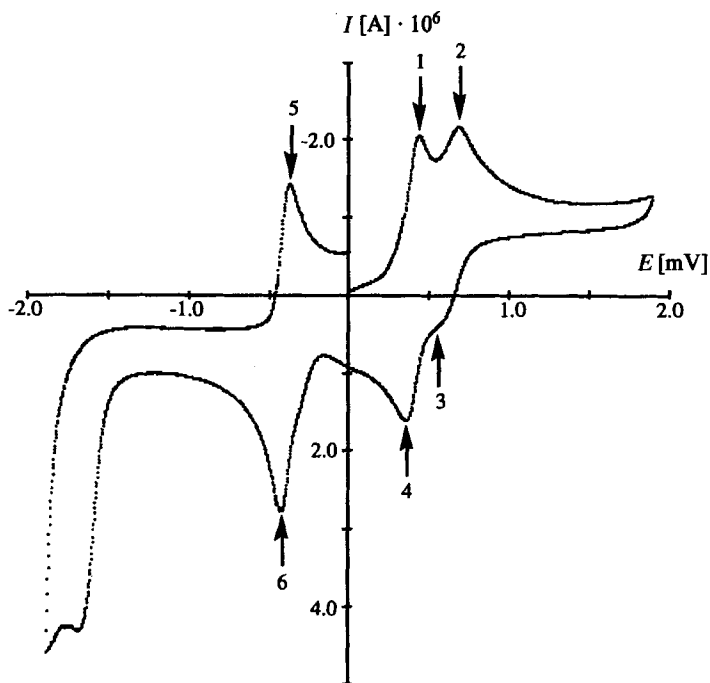


Fig. 8. Cyclic voltammogram of **13b** in acetonitrile. Peaks 5 and 6 originate from the ferrocene/ferrocenium couple, used for calibration purpose.

Table 7. Half-Wave Potentials vs. NHE from the CV of the Dinuclear Cu^{2+} Complexes **12**, **13a**, **13b**, and **14c**

	Ligand	Z	$E_{1/2(a)}$ [mV]	$E_{1/2(b)}$ [mV]	$\Delta E(a)$ [mV]	$\Delta E(b)$ [mV]
12	7	azide	-329	-549	150	90
13a	10	azide	-200	-449	63	72
14c ³⁾	11	azide	+211	-41	63	125
13b	10	1 <i>H</i> -pyrazol-1-ide	-402	-635	85	132

In the series of the bis-macrocycles **7**, **10**, and **11**, the number of S-atoms is steadily increasing, whereas the number of N-atoms decreases. This makes the ligand 'softer' and more prone to stabilize the Cu^{I} over the Cu^{II} oxidation state. In the azide-bridged complexes **12**, **13a**, and **14c**³⁾, the potential is shifted by more than 500 mV to more positive values. Besides this, the potentials are also determined by the nature of the bridging ligand. The dinuclear Cu^{2+} complex of **10** with azide as a bridging group has a more positive potential than that with 1*H*-pyrazol-1-ide (**13a** vs. **13b**, see Table 7).

In conclusion, we can say that this new type of bis-macrocycles, consisting of two cyclononane rings with N and S as donor group and a pyrazole moiety as bridging unit, can form dinuclear metal complexes with Cu^{2+} and Ni^{2+} , in which the intermetallic distance can be modulated by the nature of the exogenous bridging ligand. In addition,

³⁾ Complex **14c** was prepared by mixing the ligand **11** with 2 equiv. of Cu^{2+} and 1 equiv. of azide, by adjusting the pH to 5 and by evaporating the aqueous solution to dryness.

we have shown that the redox potential of the Cu^{2+} complexes can be controlled either by the number of S-donors in the macrocycle or by the nature of the exogenous bridging ligand. Although their reactivity was not yet tested, these compounds can be regarded as structural models for metalloproteins.

We thank Prof. R. Nesper, ETH, Zürich, for the determination of the temperature dependence of the magnetic susceptibility. This work was supported by the Swiss National Science Foundation (project No. 20-45408.95), and this is gratefully acknowledged.

REFERENCES

- [1] R. Kowallick, M. Neuburger, M. Zehnder, Th. A. Kaden, *Helv. Chim. Acta* **1997**, *80*, 948.
- [2] 'Copper Coordination Chemistry: Biochemical and Inorganic Perspectives', Eds. K. Karlin and J. Zubieta, Academic Press, New York, 1983; 'Biological and Inorganic Copper Chemistry', Eds. K. Karlin and J. Zubieta, Academic Press, New York, 1986, Vols. I and II.
- [3] K. A. Magnus, H. Ton-That, J. E. Carpenter, *Chem. Rev.* **1994**, *94*, 727; J. Ling, L. P. Nestor, R. S. Czernuszewicz, T. G. Spiro, R. Fraczkiewicz, K. D. Sharma, T. M. Loehr, J. Sanders-Loehr, *J. Am. Chem. Soc.* **1990**, *112*, 9548.
- [4] J. L. Cole, P. A. Clark, E. J. Solomon, *J. Am. Chem. Soc.* **1994**, *116*, 7682.
- [5] A. Messerschmidt, H. Luecke, R. Huber, *J. Mol. Biol.* **1993**, *230*, 997.
- [6] J. A. Tainer, E. D. Getzoff, J. S. Richardson, D. C. Richardson, *Nature (London)* **1983**, *306*, 284; A. Gärtner, U. Weser, *Topics Curr. Chem.* **1986**, *132*, 1; E. G. Cass, in 'Metalloproteins, Part 1', VCH Publishers, Weinheim, 1985, p. 121; I. Fridovich, *J. Biol. Chem.* **1989**, *264*, 7761.
- [7] E. Bouwman, W. L. Driessen, J. Reedijk, *Coord. Chem. Rev.* **1990**, *104*, 143; N. Kitajima, Y. Morooka, *Chem. Rev.* **1994**, *94*, 737; E. I. Solomon, M. J. Baldwin, M. D. Lowery, *ibid.* **1992**, *92*, 521; E. Spodine, J. Manzur, *Coord. Chem. Rev.* **1992**, *119*, 171.
- [8] W. D. Carlisle, D. E. Fenton, P. B. Roberts, U. Castellato, P. A. Vigato, *Transition Met. Chem.* **1986**, *11*, 292; M. G. B. Drew, A. Lavery, V. Mckee, S. M. Nelson, *J. Chem. Soc., Dalton Trans.* **1985**, 1771; J. Jazwinski, J. M. Lehn, D. Liliensbaum, R. Ziessle, J. Giulhem, *J. Chem. Soc., Chem. Commun.* **1987**, 1691; R. Menif, J. Reibenspies, A. E. Martell, *Inorg. Chem.* **1991**, *30*, 3446; A. Lavery, S. M. Nelson, M. G. B. Drew, *J. Chem. Soc., Dalton Trans.* **1987**, 2975; S. S. Tandon, L. K. Thompson, J. N. Bridson, *Inorg. Chem.* **1993**, *32*, 32; M. G. B. Drew, M. McCann, S. M. Nelson, *J. Chem. Soc., Chem. Commun.* **1979**, 481; S. M. Nelson, *Pure Appl. Chem.* **1980**, *52*, 2461; J. M. Lehn, *ibid.* **1980**, *52*, 2441.
- [9] Th. A. Kaden, in 'Transition Metals in Supramolecular Chemistry', Eds. L. Fabrizzi and A. Poggi, Kluwer Academic Publishers, Dordrecht, 1994, p. 211.
- [10] S. S. Tandon, L. K. Thompson, J. N. Bridson, V. Mckee, A. J. Downard, *Inorg. Chem.* **1992**, *31*, 4635.
- [11] L. Behle, M. Neuburger, M. Zehnder, Th. A. Kaden, *Helv. Chim. Acta* **1995**, *78*, 693.
- [12] G. R. Weisman, D. J. Vachon, V. B. Johnson, D. A. Gronbeck, *J. Chem. Soc., Chem. Commun.* **1987**, 886.
- [13] J. C. A. Boeyens, S. M. Dobson, R. D. Hancock, *Inorg. Chem.* **1985**, *24*, 3073; P. Hoffmann, A. Steinhoff, R. Mattes, *Z. Naturforsch. B: Chem. Sci.* **1987**, *42*, 867.
- [14] T. G. Schenck, J. Downes, C. R. C. Milne, P. B. Mackenzie, M. Boucher, J. Whealan, B. Bosnich, *Inorg. Chem.* **1985**, *24*, 2334.
- [15] A. S. Craig, R. Katakya, R. Matthews, D. Parker, *J. Chem. Soc., Perkin Trans. 2* **1990**, *9*, 1523; A. Mc Auley, S. Subramanian, *Inorg. Chem.* **1990**, *29*, 2830.
- [16] A. Altomare, G. Cascarano, G. Giacovazzo, A. Guagliardi, M. C. Burla, G. Polidori, M. Camalli, *J. Appl. Crystallogr.* **1994**, *27*, 435.
- [17] D. Watkin, R. Carruthers, P. Betteridge, 'CRYSTALS', Chemical Crystallography Laboratory, Oxford, 1990.
- [18] 'International Tables for Crystallography', Kynoch Press, Birmingham, 1974. Vol. IV.
- [19] O. Kahn, 'Molecular Magnetism', VCH Publishers, Weinheim, 1993, p. 3.
- [20] D. Hanke, K. Wiegard, B. Nuber, R. S. Lu, R. K. McMullen, T. F. Koetzle, R. Bau, *Inorg. Chem.* **1993**, *32*, 4300.
- [21] B. Bleaney, K. D. Bowers, *Proc. R. Soc. London [Ser.] A* **1952**, *214*, 451.
- [22] J. B. Flanagan, S. Margel, A. J. Bard, F. C. Anson, *J. Am. Chem. Soc.* **1978**, *100*, 4248.
- [23] J. R. Carruthers, D. J. Watkin, *Acta Crystallogr., Sect. A* **1979**, *35*, 698.